Geophysical Research Letters

RESEARCH LETTER
10.1029/2022GL100028

Key Points:

- A Pleistocene accelerated exhumation is identified within the Sumatran fault zone
- The Barisan Mountains may have experienced uplift and rapid exhumation in the late Miocene to Pliocene
- Forearc faults likely accommodated early oblique plate motion and deformation relocated to the Sumatran fault around 2 Ma

Supporting Information:

Supporting Information may be found in the online version of this article.

Correspondence to:

Y. Wang,
wangyang26@mail.sysu.edu.cn

Citation:

Wang, Y., Gao, Y., Morley, C. K., Seagren, E. G., Qian, X., Rimando, J. M., et al. (2023). Pleistocene accelerated exhumation within the Sumatran fault: Implications for late Cenozoic evolution of Sumatra (Indonesia). *Geophysical Research Letters*, *50*, e2022GL100028. https://doi.org/10.1029/2022GL100028

Received 15 JUN 2022
Accepted 6 JAN 2023

Pleistocene Accelerated Exhumation Within the Sumatran Fault: Implications for Late Cenozoic Evolution of Sumatra (Indonesia)

Yang Wang[1,2], Yan Gao[1], Chris K. Morley[3], Erin G. Seagren[4], Xin Qian[1,2], Jeremy M. Rimando[5], Peizhen Zhang[1,2], and Yuejun Wang[1,2]

[1]Guangdong Provincial Key Laboratory of Geodynamics and Geohazards, School of Earth Sciences and Engineering, Sun Yat-sen University, Guangzhou, China, [2]Southern Marine Science and Engineering Guangdong Laboratory (Zhuhai), Zhuhai, China, [3]PTT Exploration and Production, Bangkok, Thailand, [4]School of Environmental Science, Simon Fraser University, Burnaby, BC, Canada, [5]School of Earth, Environment & Society, McMaster University, Hamilton, ON, Canada

Abstract The 1,900-km-long Sumatran fault plays an important role in accommodating oblique plate motion between the Indo-Australian and Sunda plates. Although fault geometry, kinematics, and seismic activity are well-studied, the onset of dextral motion on the Sumatran fault and uplift of adjacent Barisan Mountains is unclear; this hinders an understanding of the late Cenozoic evolution of Sumatra and the forearc region. In this study, we use low-temperature thermochronology to measure cooling histories of rocks within and outside of the Sumatran fault. An accelerated exhumation within the fault zone began at ~2 Ma. The Barisan Mountains may have experienced uplift and associated river incision in the late Miocene to Pliocene. The fault systems in the forearc region were inferred to be kinematically linked to the Andaman Sea and Sunda Strait and accommodated early relative plate convergence, then relocated the strike-slip component of deformation to the Sumatran fault at ~2 Ma.

Plain Language Summary The 1,900-km-long trench-parallel Sumatran fault plays an important role in accommodating the oblique plate motion between the Indian Ocean lithosphere and Sunda continental crust. Although fault geometry, kinematics, and seismic activity are well-studied, the onset of motion on the Sumatran fault and uplift of adjacent Barisan Mountains is unclear, hindering an understanding of the late Cenozoic evolution of Sumatra and forearc region. Fault movement with dip-slip components affects bedrock exhumation rates of the fault zone, which should be recorded by low-temperature thermochronologic data. We present new apatite and zircon (U-Th)/He data collected from the Sumatran fault zone and adjacent Barisan Mountains to examine their exhumation histories, which has previously been unconstrained. We then discuss the driving mechanism based on structural, sedimentary and chronologic observations. Our AHe and ZHe data help to provide timing constraints on the late Cenozoic tectonic and landscape evolution of the Sumatran fault and Barisan Mountains, which in turn can be related to broader plate tectonic setting.

1. Introduction

Oblique subduction of the Indo-Australian plate below the Sunda continental crust generated one of the most striking subduction zones in the world, which extends >5,000 km from Myanmar (NW) to Sumba Island (SE; Figure 1a). This plate boundary produces numerous major destructive earthquakes, including the 2004 Indian Ocean earthquake (Mw 9.1–9.3; Ammon et al., 2005). The 1900-km-long Sumatran fault traverses Sumatra (Indonesia) and runs parallel to the Sumatra Trench in the central part of the Sunda subduction zone (Figure 1b; e.g., McCaffrey, 1991, 2009; Sieh & Natawidjaja, 2000; Yeats et al., 1997). Northwards, the Sumatra fault links with the dextral pull-apart system in the Andaman Sea (the Central Andaman Basin spreading center), and curves south toward the Sumatra Trench at its southern end (Figure 2a; Curray et al., 1979; Huchon & LePichon, 1984; Curray, 2005). During the past half century, the Sumatran fault has been widely cited as a typical example of slip partitioning of oblique plate convergence, with a dip-slip (trench-normal slip) on the Sunda megathrust along the trench and a dextral slip component (trench-parallel slip) on the Sumatran fault in the overriding plate (Fitch, 1972; McCaffrey, 1991; Sieh & Natawidjaja, 2000). Due to this role in accommodating high oblique relative plate motion, the Sumatran fault ranks as one of the most seismogenic faults in the world (e.g., Natawidjaja, 2018; Sieh & Natawidjaja, 2000).

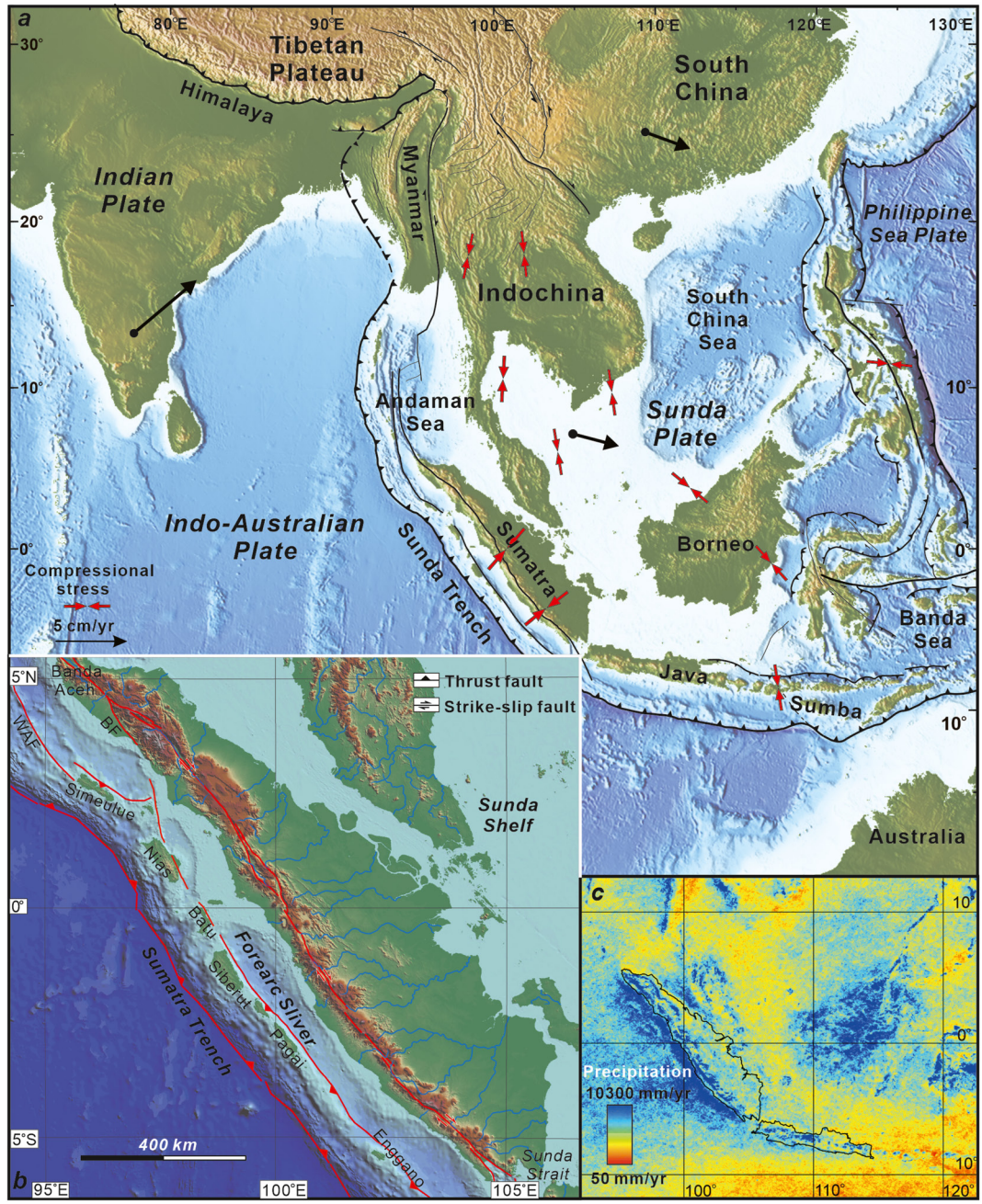

Figure 1. Main tectonic boundaries in SE Asia at the convergence zone of the Eurasian, Philippine Sea, and Indo-Australian Plates. The island of Sumatra is situated along the southwestern margin of the Sunda plate. Black arrows represent absolute plate motions (Simons et al., 2007). Red arrows indicate present-day maximum horizontal stress orientations (Tingay et al., 2010). (b) Topographic map of Sumatra and adjacent regions. A chain of islands formed forearc ridge between the trench and Sumatra. The Barisan Mountains delineate the entire southwestern margin of Sumatra. The Sumatran fault extends southeast from Banda Aceh in north, traverses the Barisan Mountains, and terminates at the Sunda Strait. (c) The mean annual precipitation from TRMM 2B31 (1998–2009, processed by B. Bookhagen) in the study area.

Previous geological and geophysical observations have focused on the geometry, kinematics, and seismic activity of the Sumatran fault. It has a sinusoidal trace (amplitude ~55 km) and is atypically segmented for a strike-slip fault (e.g., Bellier et al., 1997; Natawidjaja, 2018; Sieh & Natawidjaja, 2000). GPS observations suggest an increase of slip rates from ~6 mm/yr near the Sunda Strait in the south to 16–26 mm/yr in the central and northern fault segments (Figure 2b; Bellier & Sébrier, 1995; Genrich et al., 2000, Ito et al., 2012). Geologic

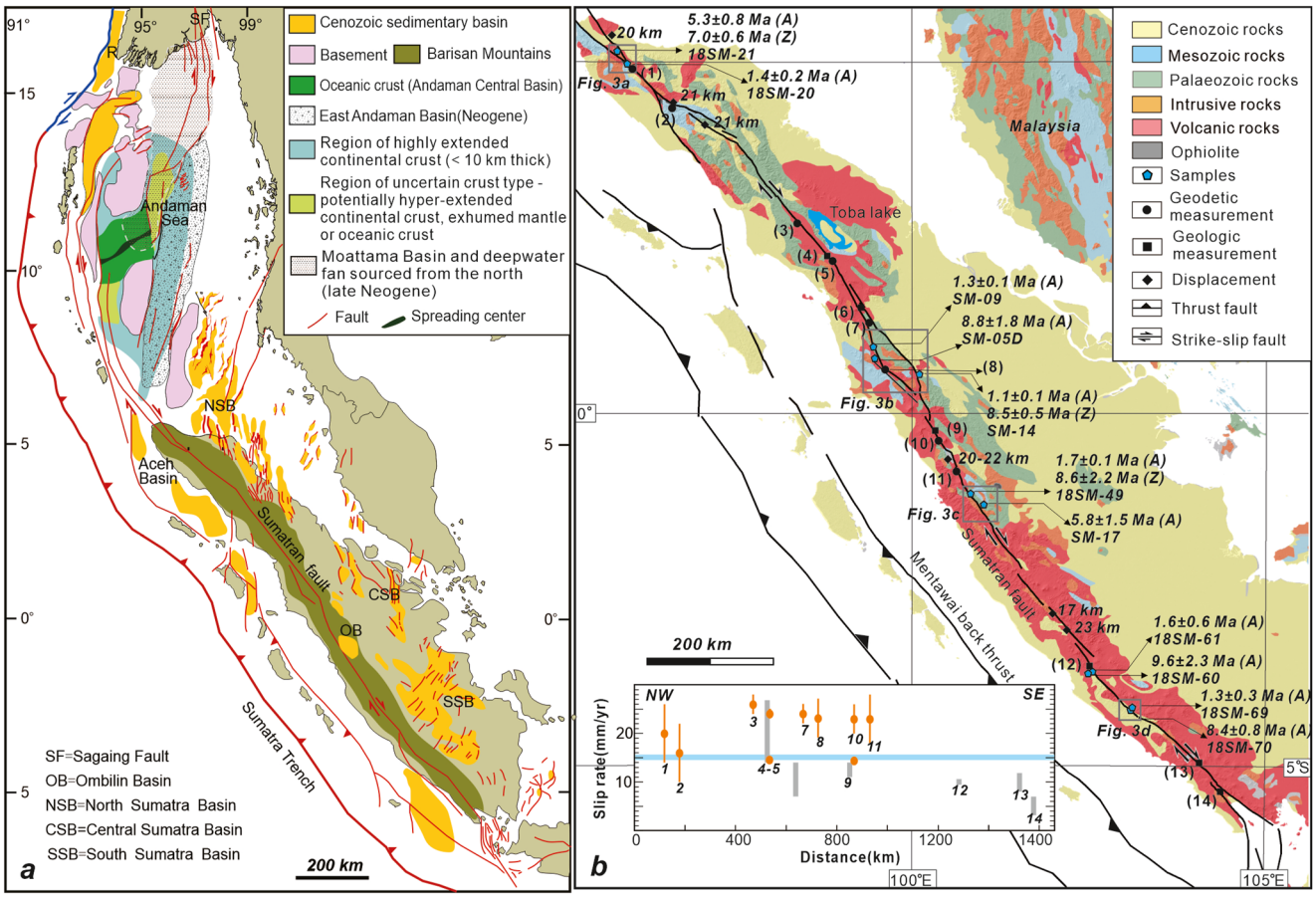

Figure 2. (a) Regional map showing the Neogene tectonic elements of Sumatra and the Andaman Sea (after Morley et al., 2022; Pubellier & Morley, 2014). (b) Geologic map of Sumatra and adjacent regions. The insets are slip rates along the strike of the Sumatran fault, collected from previous studies ([1, 2] Ito et al., 2012; [3, 7, 8, 11] Genrich et al., 2000; [4, 12] Sieh et al., 1994; Bradley et al., 2017; [5] Genrich et al., 2000, Bradley et al., 2017; [6] Hickman et al., 2004; [9] Sieh et al., 1994; Bradley et al., 2017; [10] Genrich et al., 2000 Bradley et al., 2017; [13, 14] Natawidjaja et al., 2017).

slip rates based on offset rivers incised into young volcanic tuffs of known ages are generally consistent with the northwestward increasing trend but differ in detail (e.g., McCaffrey, 2009; Natawidjaja et al., 2017; Sieh & Natawidjaja, 2000). It is noteworthy that the Sumatran fault and kinematically-linked Andaman Sea and Sunda Strait do not exhibit synchronous timing of activity and amount of displacement. In the past 11 Myr, there has been 460 km of spreading in the Andaman Sea, with average rates of ~37 mm/yr (Curray et al., 1979). However, more recent studies suggest that the spreading could be predominantly of Pliocene-Holocene age (e.g., Raju et al., 2004), while Morley and Alvey (2015) have argued for episodic spreading with a Pleistocene hiatus. The stretching of the Sunda Strait at the southern fault terminus initiated ~5 Ma ago, with a maximum displacement of 50–70 km (Lassal et al., 1989). This suggests the Sumatran fault could have initiated in the late Miocene to Pliocene. However, total displacements of ~20 km onshore and measured slip rates point to a much later onset of dextral fault movement (Sieh & Natawidjaja, 2000). Our understanding of this discrepancy is limited by insufficient timing constraints on the late Cenozoic deformation history of the Sumatran fault.

The apatite and zircon (U-Th)/He (AHe and ZHe) thermochronometric systems have low closure temperatures of 60–80°C and ~180°C (e.g., Farley, 2000; Guenthner et al., 2013) and are useful for deciphering tectonic and landscape evolution by quantifying timing, rates, and spatial patterns of rock exhumation (e.g., Herman et al., 2013; Stockli et al., 2000). In this study, we present new low-temperature thermochronology from the Sumatran fault zone and adjacent Barisan Mountains to examine their exhumation histories, which have previously been unconstrained. We then discuss potential driving mechanisms based on structural, sedimentary, and chronologic analyses. Our AHe and ZHe data provide timing constraints on the evolution of the Sumatran fault and Barisan Mountains, which can be related to the broader plate tectonic setting.

2. Geologic Setting

The island of Sumatra is situated along the southwestern margin of the Sunda plate, which overrides the subducting Indo-Australian oceanic plate (Figure 1a). Trench-parallel faults, such as subduction thrusts and strike-slip faults, accommodate 50–70 mm/yr of relative motion between the two obliquely converging plates (e.g., McCaffrey, 1992; Prawirodirdjo et al., 2000; Sieh & Natawidjaja, 2000). A narrow crustal wedge (forearc sliver), bound by the Sumatran fault to the northeast and Sumatra Trench to the southwest, shows evidence for a northward increase in slip vector (Figure 1b; Genrich et al., 2000; McCaffrey, 2009); otherwise, the forearc is interpreted to behave as a rigid block (Bradley et al., 2017). Furthermore, a series of offshore faults, such as the Mentawai and Batee faults, developed in the forearc region and accommodated oblique motion, though their deformation history and kinematics are unclear (Figure 1b; Diament et al., 1992; Sieh & Natawidjaja, 2000).

A chain of islands including the Simeulue, Nias, Batu, Siberut, Pagai, and Enggano islands formed along the non-volcanic forearc ridge between the trench and Sumatra (Figure 1b; Harbury & Kallagher, 1991; McCaffrey, 2009). Structural deformation and outcropping rocks on these islands suggest that they resulted from the uplift and thickening of the incoming oceanic crust and formation of an accretionary prism (McCaffrey, 2009; Moore & Curray, 1980). The 100-km-wide Barisan Mountains delineate the entire southwestern margin of Sumatra (Figure 1b). Major lithologies exposed in the mountain ranges include Precambrian basement and Palaeozoic-Mesozoic strata which are variably metamorphosed and deformed, granites with a wide range of isotopic ages, and widespread Cenozoic volcanic rocks (Figure 2b; e.g., Barber et al., 2005). Active volcanoes run along the crest of the Barisan Mountains, adjacent to the Sumatran fault, though whether or not magmatism has influenced fault formation is controversial (Bellier & Sébrier, 1994; Sieh & Natawidjaja, 2000).

The Sumatran fault extends southeast from Banda Aceh in north Sumatra, traverses the Barisan Mountains, and terminates at the Sunda Strait (Figure 1b; e.g., Natawidjaja, 2018; Sieh & Natawidjaja, 2000). The largest irregularity in the fault trace is the Equatorial Bifurcation where two fault strands are offset by about 35 km (Sieh & Natawidjaja, 2000). The fault consists of 20 major segments with lengths ranging from 35 to 200 km (e.g., Bellier et al., 1997; Bradley et al., 2017; Natawidjaja, 2018; Sieh & Natawidjaja, 2000). Over 12 discontinuities in the fault trace have been identified; most are releasing, right-stepping geometries, but a few restraining, left-stepping features are present (Sieh & Natawidjaja, 2000). In addition, pull-apart depressions, linear valleys, escarpments, and deflected streams are well developed along strike, indicating active right-lateral faulting with dip-slip components (e.g., Bellier et al., 1997; Natawidjaja, 2018; Sieh & Natawidjaja, 2000). Based on offsets of geologic and geomorphic features, Sieh and Natawidjaja (2000) suggested that the total onshore displacement of the Sumatran fault is ~20 km. Measurements of slip rates vary depending on different methods and change spatially along strike (Figure 2b), which is discussed below in the context of fault evolution. Given rapid relative plate motion, Sumatra experiences frequent earthquakes, including thrust earthquakes, strike-slip earthquakes on the Sumatran fault, volcanic earthquakes, and deep earthquakes within the subducting lithosphere (McCaffrey, 2009).

3. (U-Th)/He Thermochronology

3.1. Methodology

Eleven samples were collected for (U-Th)/He thermochronologic analysis, including granitoids, sandstone, and volcanic rocks from the Sumatran fault zone and adjacent Barisan Mountains (Figure 2b and Figure S1 in Supporting Information S1). After crushing, heavy liquid and magnetic separation, three to four euhedral apatite and zircon grains that were non-fractured and free of inclusions, were selected and measured. Analytical work was conducted at the State Key Laboratory of the Institute of Geology, China Earthquake Administration. Detailed procedures are described in Wang et al. (2019). All reported grain ages are alpha-ejection corrected (Farley et al., 1996). We calculated the mean age and standard deviation for the spread of replicate analyses. ZHe and/or AHe data in each sample were modeled to explore the time-temperature histories using QTQt—a Bayesian transdimensional Markov chain Monte Carlo method (Gallagher, 2012). We do not set initial temperature constraints for samples which have both ZHe and AHe data, while the initial constraints were set at 100 ± 20°C during 10-4 Ma for other samples within the fault zone based on older AHe ages at nearby sites. All model results are based on 100,000 iterations: 50,000 for the inversion process burn-in and 50,000 to calculate the posterior ensemble (Gallagher, 2012). The "expected model" results we describe are weighted by the posterior probability of each individual thermal history.

3.2. Thermochronologic and Thermal Modeling Results

Most grain AHe and ZHe ages are less than 10 Ma (Tables S1 and S2 in Supporting Information S1). There is no clear correlation between single-grain (U-Th)/He dates and effective uranium concentration ([eU] = [U] + 0.235 × [Th]), suggesting minimal radiation damage (Figure S2 in Supporting Information S1). Samples 18SM-21 and -20 are granodiorites collected from the northernmost segment of the Sumatran fault (Figure 3a). Sample 18SM-20, collected from a linear valley along the fault zone, exhibits a mean AHe age of 1.4 ± 0.2 Ma from four apatite grains. Conversely, sample 18SM-21, taken from an east-flowing river valley ~2 km away from the fault zone, has an AHe age of 5.3 ± 0.8 Ma. The ZHe age of this sample is slightly older (7.0 ± 0.6 Ma, Figure 2b). The Sumatran fault bifurcates into two strands near the equator (Figure 3b). The western branch strikes N20-30°W and turns to N45°W in the south, forming a releasing bend. Sample SM-09 was collected near the western flank of the pull-apart basin, where the dextral normal fault has generated ~1.5 km of topographic relief, and yields an AHe age of 1.3 ± 0.1 Ma (Figure 3b). Sample SM-05D was collected from granites ~5 km west of the fault zone and has three AHe grain dates between 6.6 and 10.9 Ma, with a mean age of 8.8 ± 1.8 Ma (Table S1 in Supporting Information S1 and Figure 3b). To the east of these two samples, the eastern fault branch also forms a pull-apart depression with high west-facing escarpments (Figure 3b). Sample SM-14 was taken from granites along the frontal ranges and has an AHe age of 1.1 ± 0.1 Ma and a ZHe age of 8.5 ± 0.5 Ma, respectively. In the central segment of the Sumatran fault, the fault slices through the Barisan Mountains, forming deep linear valleys and depressions (Figure 3c). Sample 18SM-49 was collected from a linear fault valley and yield an AHe age of 1.7 ± 0.1 Ma and a ZHe age of 8.6 ± 2.2 Ma. Conversely, a granite (SM-17) in a SE-flowing river valley, ~5 km away from the fault zone, yields a cooling age of 5.8 ± 1.5 Ma (Figure 3c). We collected samples 18SM-60, -61, -69, and -70 from the southern Sumatran fault, where dextral fault movements with dip-slip components have formed valleys, depressions, and escarpments along strike (Figure 3d). Samples 18SM-61 and -69, both of which were collected within the fault zone, exhibit young AHe ages of 1.6 ± 0.6 Ma and 1.3 ± 0.3 Ma, respectively. In contrast, ~2–5 km away from the fault, samples 18SM-60 and -70 have older AHe ages of 9.6 ± 2.3 Ma and 8.4 ± 0.8 Ma respectively (Figure 3d).

Thermal history modeling of four representative samples within and outside the fault zone are shown in Figures 3a–3d. The inverse modeling results for samples from the Sumatran fault zone suggest well-constrained rapid cooling beginning at ~2 Ma and continues to the present (Figures 3b–3d). Samples within and outside of the fault zone collectively indicate that a potential early cooling episode may have occurred in the late Miocene followed by slow and quiescent cooling in the Pliocene (Figures 3a–3c).

4. Discussion

4.1. Thermal History and Interpretations

Reported AHe ages display two age clusters: 1–2 Ma and 6–9 Ma. These ages and cooling histories may have been affected by magmatic reheating, climate-associated exhumation, and tectonic activity, though we exclude the former two as major causes for the reasons discussed below. First, we argue that the late Neogene and Quaternary magmatism has minor effects. Based on field investigations and the geological map of Sumatra (Barber et al., 2005), samples 18SM-20 and -21 were collected from Paleogene granodiorite. Samples SM-09 and -14 were taken from Palaeozoic sandstone, adjacent to Miocene volcanics (SM-05D, Figure 2b), which yield an AHe age ~7 Myr older than samples SM-09 and -14, suggesting these two samples have unlikely been affected by reheating. We collected samples 18SM-49 and SM-17 from Meso-Cenozoic intrusive rocks, 7–10 km away from Quaternary volcanics, and find ages of 1.7 ± 0.1 Ma and 5.8 ± 1.5 Ma; if these two samples were affected by reheating, we would expect them to have similar AHe ages. Samples 18SM-61, -60, -69, and -70 were collected from sites covered by or adjacent to Quaternary volcanic rocks (Barber et al., 2005). If these four samples were reset by Quaternary volcanism, they would exhibit similar cooling ages to the volcanism, which they do not. A climate-driven increase in erosion would cause contemporaneous regional exhumation across Sumatra; however, the cooling histories of samples within and outside of the fault zone are markedly different. In addition, while precipitation varies along strike of the Sumatran fault, the cooling ages and long-term exhumation rates of analyzed samples are not correlated with mean annual rainfall, also suggesting minimal climatic control (Figure 1c and Figure S2 in Supporting Information S1).

Fault movements with dip-slip components could affect bedrock exhumation within the fault zone, which should in turn be recorded by low-temperature thermochronologic data. All samples within the Sumatran fault give AHe

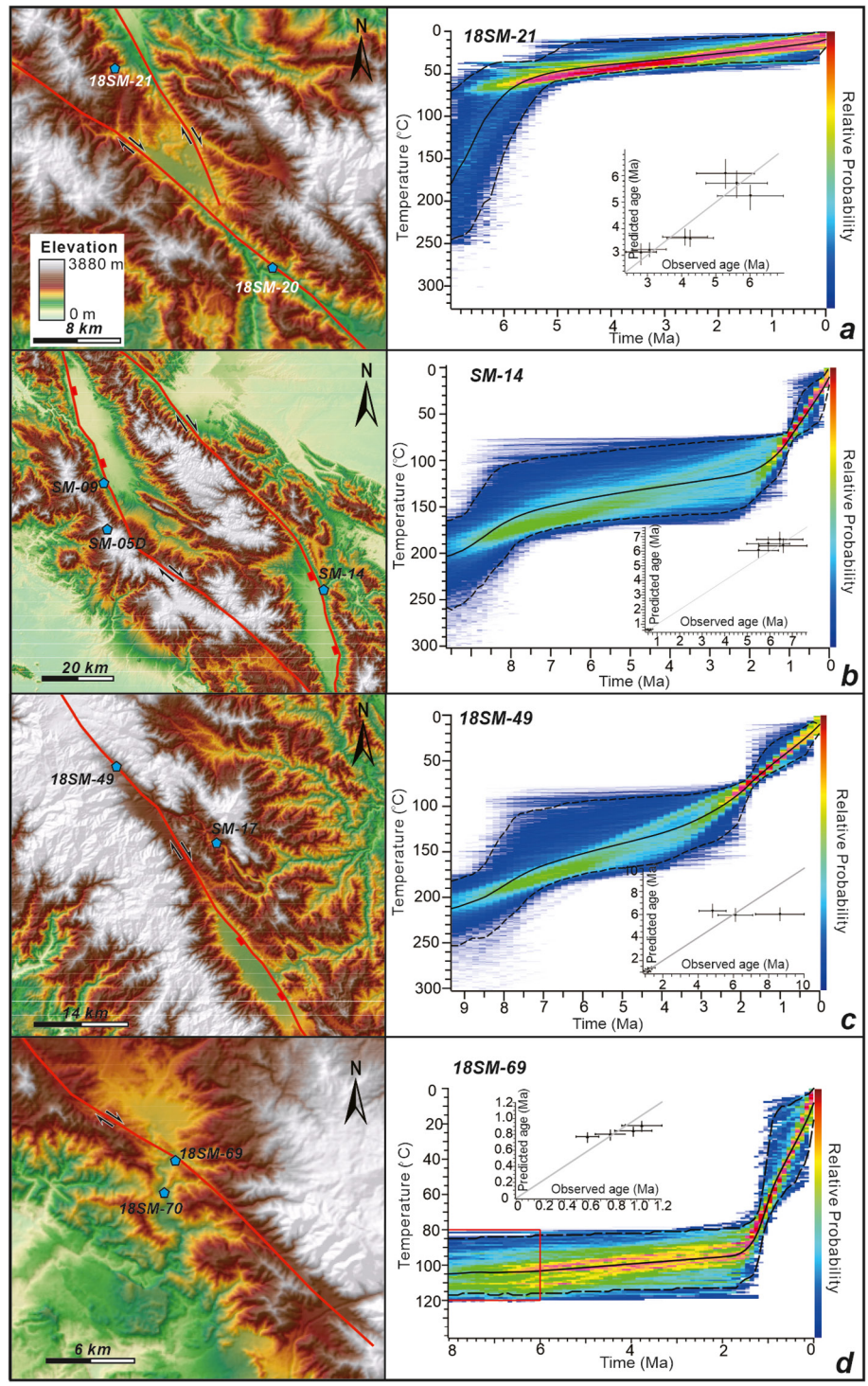

Figure 3. (a–d) Digital elevation model images showing topography of sample sites and inverse thermal modeling results derived from QTQt modeling. Color maps show conditional probability for thermal history simulations. Dashed lines correspond to 95% confidence interval for the sample. We do not set initial temperature constraints for samples 18SM-21, -49, and SM-14, while the initial constraints indicated by the red box were set at 100 ± 20°C during 10-6 Ma for sample 18SM-69 based on older AHe age at nearby site. Insets show fitness of predicted dates with respect to observed data.

cooling ages of < 2 Ma and the thermal modeling results suggest a well-constrained rapid cooling beginning at ~2 Ma (Figure 3 and Figure S3 in Supporting Information S1). Conversely, samples several kilometers away from the fault yield older AHe ages of 5–10 Ma (Figure 2b). This suggests that local fault displacements may control different spatial patterns of exhumation. The dextral movement with dip-slip components formed releasing or restraining fault bends, stepovers, pull-apart basins, and linear valleys along strike. Samples SM-09, -14, and -61 were collected from footwalls at the margins of extensional basins and give AHe ages of 1.1–1.6 Ma. The basin-bounding faults created large escarpments, with heights between hundreds of meters and ~1.5 km, suggesting a significant vertical component to fault displacement. Conversely, the AHe ages of samples SM-05D and 18SM-60, 2–5 km away from these dextral normal faults, are ~8 Myr older. We collected samples 18SM-20, -49, and -69 from deep linear fault valleys (Figure 3) and they yield similar AHe ages of 1.4 ± 0.2 Ma, 1.7 ± 0.1 Ma, and 1.3 ± 0.3 Ma. In contrast, samples outside of the fault zone give older AHe ages (18SM-21, -70, and SM-17), implying a strong structural control (Figure 3). Together with thermal modeling results and high averaged long-term exhumation rates focused in the fault zone, we suggest that the Pleistocene rapid cooling and spatially variable exhumation were caused by dextral movement with dip-slip components along the Sumatran fault.

Besides NW-striking depressions, linear valleys and ridges, nearly NE- and SW-flowing rivers that run perpendicular to the Sumatran fault have incised the Barisan Mountains. Samples 18MS-21, -70, SM-05D, and -17, collected from the floor of incised river valleys, display cooling ages ranging from 5.3 to 8.8 Ma. Sample 18SM-21, -49, and SM-14 yield ZHe ages of 7.0 to 8.6 Ma. The similar and overlapping ZHe and AHe ages likely indicate a potential rapid cooling during this period. In addition, thermal modeling of samples within and outside of the fault zone also reveal this fast cooling along the Barisan Mountains in the late Miocene (Figure 3 and Figure S3 in Supporting Information S1), which was likely caused by increased river incision during mountain building. However, due to dense vegetation cover and strong weathering, we were unable to collect vertical profiles with a large elevation span, which brings some uncertainty to this argument.

4.2. Tectonic Implications

Based on a synthesis of our new observations and existing data, we explore the late Cenozoic tectonic and landscape evolution of Sumatra and the forearc region. Rocks exposed on offshore islands southwest of Sumatra indicate that the forearc ridge formed in the late Eocene-Oligocene, though subduction may have started in the Cretaceous (~100 Ma; Curray et al., 1979; McCaffrey, 2009). These forearc-ridge islands were likely uplifted close to sea level in the early- to mid-Miocene, as indicated by shallow marine carbonate sedimentation (Harbury & Kallagher, 1991). We propose that the uplift of the Barisan Mountains may have occurred in the late Miocene to Pliocene for the following reasons. First, coarse clastic sediments from Sumatra were deposited offshore in the forearc basin at ~10 Ma, and fluvial drainage on Sumatra was predominately east-flowing prior to the Pliocene, and only switched to westward flow later (Cameron et al., 1980; Harbury & Kallagher, 1991; Karig et al., 1979). Second, the transpressional deformation occurred in the last 5 Myr or earlier, which produced large-scale folds in the major basins of Sumatra, including the Ombilin and the North, Central, and South Sumatra basins, and may have affected the Barisan Mountains (Figure 2a; e.g., Barber et al., 2005; Carrillat et al., 2013; Zaim et al., 2012). Third, paleogeographic reconstructions of SE Asia incorporating basin data, particularly palynology by Morley et al. (2016) and R. J. Morley (2018), show that Sumatra was largely covered by marine conditions until ~10 Ma when the narrow subaerial island coincident with the Barisan Mountains emerged. Between 5 and 3 Ma much of Sumatra became subaerial. Forth, our AHe and ZHe thermochronologic data, together with thermal history modeling, indicate a potential late Miocene-early Pliocene rapid exhumation episode across the Barisan Mountains, although the onset timing, rate, and magnitude are less constrained. The uplift mechanism is inferred to be associated with magma input likely due to change of subduction rate or angle (Harbury & Kallagher, 1991). Widespread Cenozoic igneous rocks across Sumatra display typical subduction-related geochemical signatures and existing argon ages show an age cluster since 6 Ma (inset in Figure 4a; e.g., Barber et al., 2005; Bellon et al., 2004 and references therein). Additionally, magmatic activity migrated from the SW coast region (near-trench position) to the Sumatran fault, as evidenced by the spatial distribution of the Paleocene-Miocene magmatic and Plio-Quaternary volcanic rocks (Bellon et al., 2004). If this is true, non-uniform uplift and exhumation would have occurred across the Barisan Mountains (Figure 4a).

The rapid exhumation within the Sumatran fault which started at ~2 Ma revealed by our (U-Th)/He data and thermal history modeling were caused by the initiation or accelerated motion of the Sumatran fault. As mentioned

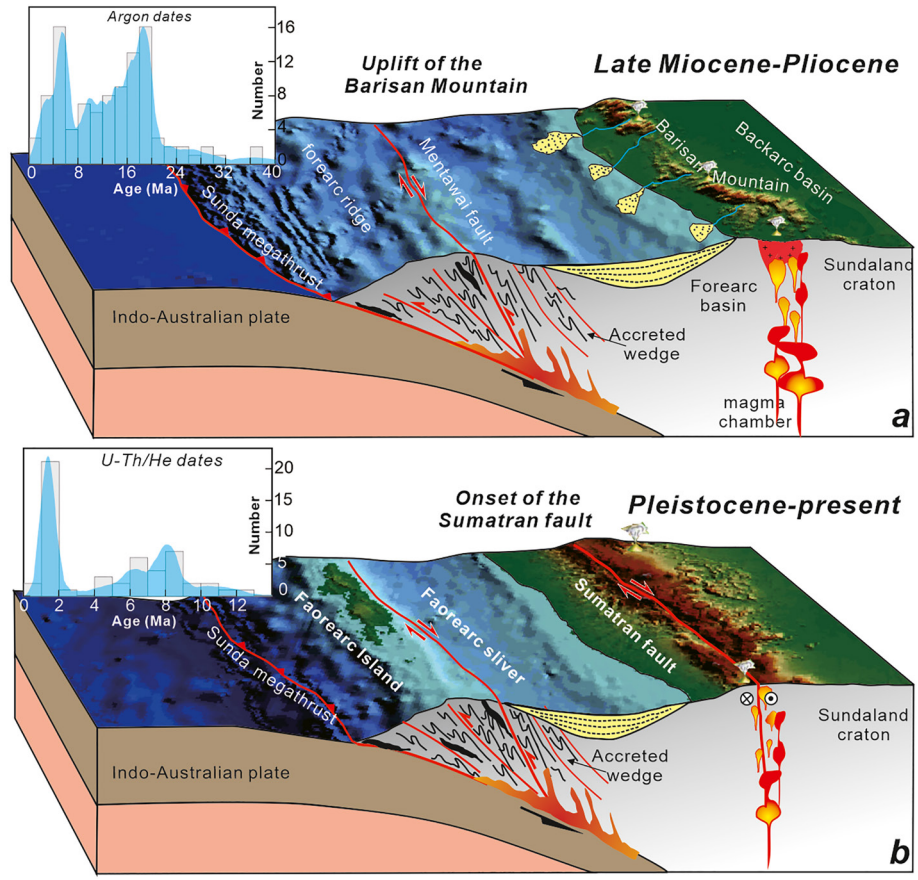

Figure 4. (a, b) Tectonic evolution of Sumatra and forearc regions. Uplift of the Barisan Mountains may have occurred in the late Miocene to early Pliocene due to magma input. The dextral strike-slip movement along the Sumatran fault likely initiated at < 2 Ma with earlier onset of fault systems in the forearc region, which were kinematically linked with the Andaman Sea and Sunda Strait. Insets are histograms of argon ages measured on Cenozoic igneous rocks (Barber et al., 2005; Bellon et al., 2004 and references therein) and (U-Th)/He grain dates of Sumatra (this study).

above, simple estimations of slip rates based on plate convergence velocities, strain partitioning, and the offset of dated geologic and geomorphic markers indicates slip rate increases from ~5.5 mm/yr in the south (5°S) to ~38 mm/yr in the north where the obliquity of subduction increases (5°–6°N; McCaffrey, 1991; see review in Bradley et al., 2017). However, more recent geodetic, geological, and numerical modeling evidence indicates a fairly consistent 15 mm/yr slip along the whole Sumatran fault, irrespective of trench curvature and obliquity (Bradley et al., 2017). Total fault displacement varies between 17 and 23 km according to offsets of Quaternary folds and rivers and the extension of pull-apart basins (Sieh & Natawidjaja, 2000). Therefore, the thermochronologic evidence, highly fault segmented nature indicative of fault immaturity, and onshore fault displacement and measured slip rates, all support Pleistocene initiation of the Sumatran fault. It could be argued that if the fault was active earlier, but in a submarine environment, then there would be little erosion, and consequently low-temperature thermochronology would not be able to detect fault movement. However, the rapid exhumation beginning around 2 Ma, occurred several million years after the Barisan Mountains emerged as an island. However, we cannot fully exclude the possibility that the dextral motion along the Sumatran fault is episodic with a late-Miocene onset, Pliocene hiatus, followed by Pleistocene accelerated motion.

Rather than suggest a definitive answer, our results indicate that the origin of the Sumatran fault in terms of adjusting oblique subduction needs to be re-evaluated. If the Sumatran fault is a late-stage addition to the configuration of the Sunda subduction system, it seems reasonable to assume that other equivalent faults, perhaps lying offshore closer to the trench, were kinematically linked with the Andaman Sea and Sunda Strait and potentially accommodated late Miocene-Pliocene plate convergence. Some large faults have been identified in the forearc area, such as the Mentawai and West Andaman faults (e.g., Berglar et al., 2017; Malod & Kemal, 1996; Mukti

et al., 2021; Figure 3b). The West Andaman fault is active today due to seismicity, and its onset of displacement could pre-date 5.9 Ma (e.g., Dasgupta et al., 2005; Diehl et al., 2013; Morley & Alvey, 2015). However, the amount of strike-slip displacement on these faults is disputed and is likely to be considerably less than the displacement magnitudes required for accommodation of oblique plate motion (Mukti et al., 2021).

Another key question is what caused the initiation or accelerated motion of the Sumatran fault in the Pleistocene? The fault is likely associated with a phase of compressional deformation that affected major sedimentary basins and the volcanic arc of Sumatra, including the forearc basin (Mukti et al., 2021). Regionally, the Miocene and particularly the mid-Miocene-Present marks a switch from regional extension to compression in SE Asia, which primarily reflects changes in the forces applied to the plate boundaries due to the Australia-Sundaland collision (Pubellier & Morley, 2014). The late Neogene compression of Sumatra is part of this regional trend, but the relatively late onset of deformation suggests that more local effects (e.g., slab dip, subduction rates, or the nature of the downgoing slab) also played a role. Another factor to consider is subduction-related magmatism along the Barisan Mountains, which started in the late Eocene-Oligocene or earlier (Bellon et al., 2004; Hamilton, 1974), and may have rheologically weakened the crust and controlled the formation of the Sumatran fault when fault zone properties such as strength, permeability, porosity, and hydrothermal fluids exceeded a threshold.

5. Conclusions

The Sumatran fault and structures in the forearc regions are key components of the oblique convergence zone between the Indo-Australian and Sunda plates. Our new thermochronologic data reveal a rapid exhumation stage within the Sumatran fault zone beginning at ∼2 Ma and continuing to the present, indicating that the dextral fault movements with dip-slip components may have commenced or accelerated in the Pleistocene. The Barisan Mountains, which span the entire length of the island, likely exhumed since the late Miocene due to regional uplift and associated river incision. Our new data and existing observations indicate that forearc fault systems may have accommodated early relative plate motion and the strike-slip component of deformation relocated to the Sumatran fault at ∼2 Ma, supporting the model of eastward propagating deformation from the forearc to Sumatra.

Data Availability Statement

All data used in this study are available in the Supporting Information S1 and archived in the Figshare (https://doi.org/10.6084/m9.figshare.21842250.v1).

Acknowledgments
We sincerely thank two anonymous reviewers for the thorough and critical reviews. We also thank Editor Lucy Flesch for editorial handling and constructive comments. This research was supported by National Natural Science Foundation of China (42272247, 42030301, 41830211, 41976197, 42072256) and the Second Tibetan Plateau Scientific Expedition and Research Program (STEP, 2019QZKK0703). We thank Dr Ying Wang and Xiaorong Li for (U-Th)/He analysis.

References

Ammon, C., Ji, C., Thio, H. K., Robinson, D., Ni, S., Hjorleifsdottir, V., et al. (2005). Rupture process of the 2004 Sumatra-Andaman earthquake. *Science*, *308*(5725), 1133–1139. https://doi.org/10.1126/science.1112260

Barber, A. J., Crow, M. J., & Milsom, J. S. (2005). Sumatra: Geology, resources and tectonic evolution. *Geological Society London Memoirs*, *31*(31), 234–259. https://doi.org/10.1144/gsl.mem.2005.031.01.14

Bellier, O., & Sébrier, M. (1994). Relationship between tectonism and volcanism along the Great Sumatran fault zone deduced by SPOT image analyses. *Tectonophysics*, *233*(3), 215–231. https://doi.org/10.1016/0040-1951(94)90242-9

Bellier, O., & Sébrier, M. (1995). Is the slip rate variation on the Great Sumatran Fault accommodated by forearc stretching? *Geophysical Research Letters*, *22*(15), 1969–1972. https://doi.org/10.1029/95gl01793

Bellier, O., Sébrier, M., Pramumijoyo, S., Beaudouin, T. H., Harjono, H., Bahar, I., & Forni, O. (1997). Paleoseismicity and seismic hazard along the Great Sumatran fault (Indonesia). *Journal of Geodynamics*, *24*(1–4), 169–183. https://doi.org/10.1016/s0264-3707(96)00051-8

Bellon, H., Maury, R. C., Soeria-Atmadja, R., Cotten, J., Polvé, M., & Polvé, M. (2004). 65 My-long magmatic activity in Sumatra (Indonesia), from Paleocene to present. *Bulletin de la Societe Geologique de France*, *175*(1), 61–72. https://doi.org/10.2113/175.1.61

Berglar, K., Gaedicke, C., Ladage, S., & Thole, H. (2017). The Mentawi forearc sliver off Sumatra: A model for a strike-slip duplex at a regional scale. *Tectonophysics*, *710/711*, 225–231. https://doi.org/10.1016/j.tecto.2016.09.014

Bradley, K., Feng, L., Hill, E. M., Natawidjaja, D. H., & Sieh, K. (2017). Implications of the diffuse deformations of the Indian Ocean lithosphere for slip partitioning of oblique plate convergence in Sumatra. *Journal of Geophysical Research: Solid Earth*, *122*(1), 572–591. https://doi.org/10.1002/2016jb013549

Cameron, N., Clarke, M., Aldiss, D., Aspden, J., & Djunuddin, A. (1980). The geological evolution of northern Sumatra. In *Paper presented at proceedings, 9th Indonesian petroleum association annual convention* (pp. 149–187).

Carrillat, A., Bora, D., Dubois, A., Kusdiantoro, F., Yudho, S., Wibowo, E., et al. (2013). Integrated regional interpretation and new insight on petroleum system of South Sumatra Basin, Indonesia. In *Asia pacific oil and gas conference and exhibition, APOGCE 2013* (Vol. 1, pp. 737–744). Society of Petroleum Engineers.

Curray, J. R. (2005). Tectonics of the Andaman Sea region. *Journal of Asian Earth Sciences*, *25*(1), 187–232. https://doi.org/10.1016/j.jseaes.2004.09.001

Curray, J. R., Moore, D. G., Lawver, L. A., Emmel, F. J., Raitt, R. W., Henry, M., & Kieckhefer, R. (1979). Tectonics of the Andaman Sea and Burma: Convergent margins. In J. S. Watkins, L. Montadert, & P. W. Dickenson (Eds.), *Geological and geophysical investigations of continental margins*, *American association of petroleum geologists memoir* (Vol. 29, pp. 189–198).

Dasgupta, S., Mukhopadhyay, B., & Acharyya, A. (2005). Aftershock propagation characteristics during the first three hours following the 26th December 2004 Sumatra-Andaman earthquake. *Gondwana Research*, *8*(4), 585–588. https://doi.org/10.1016/s1342-937x(05)71158-8

Diament, M., Harjono, H., Karta, K., Deplus, C., Dahrin, D., Jr., Zen, M. T., et al. (1992). Mentawai fault zone off Sumatra: A new key to the geodynamics of western Indonesia. *Geology*, *20*(3), 259–262. https://doi.org/10.1130/0091-7613(1992)020<0259:mfzosa>2.3.co;2

Diehl, T., Waldhauser, F., Cochran, J. R., Kamesh Raju, K. A., Seeber, L., Schaff, D., & Engdahl, E. R. (2013). Back-arc extension in the Andaman Sea: Tectonic and magmatic processes imaged by high-precision teleseismic double-difference earthquake relocation. *Journal of Geophysical Research: Solid Earth*, *118*(5), 2206–2224. https://doi.org/10.1002/jgrb.50192

Farley, K. A. (2000). Helium diffusion from apatite: General behavior as illustrated by Durango fluorapatite. *Journal of Geophysical Research*, *105*(B2), 2903–2914. https://doi.org/10.1029/1999jb900348

Farley, K. A., Wolf, R. A., & Silver, L. T. (1996). The effects of long alpha-stopping distances on (U-Th)/He ages. *Geochimica et Cosmochimica Acta*, *60*(21), 4223–4229. https://doi.org/10.1016/s0016-7037(96)00193-7

Fitch, T. J. (1972). Plate convergence, transcurrent faults and internal deformation adjacent to Southeast Asia and the western Pacific. *Journal of Geophysical Research*, *77*(23), 4432–4460. https://doi.org/10.1029/jb077i023p04432

Gallagher, K. (2012). Transdimensional inverse thermal history modelling for quantitative thermochronology. *Journal of Geophysics Research*, *117*(B02), 408.

Genrich, J. F., Bock, Y., McCaffrey, R., Prawirodirdjo, L., Stevens, C. W., Puntodewo, S. S. O., et al. (2000). Distribution of slip at the northern Sumatran fault system. *Journal of Geophysical Research*, *105*, 28327–28341.

Guenthner, W. R., Reiners, P. W., Ketcham, R. A., Nasdala, L., & Giester, G. (2013). Helium diffusion in natural zircon: Radiation damage, anisotropy, and the interpretation of zircon (U-Th)/He thermochronology. *American Journal of Science*, *313*(3), 145–198. https://doi.org/10.2475/03.2013.01

Hamilton, W. (1974). *Earthquake map of the Indonesian regio*n. USGS Miscellaneous Investigations Series. Map I-875C.

Harbury, N. A., & Kallagher (1991). The Sunda outer-arc ridge, north Sumatra, Indonesia. *Journal of Southeast Asian Earth Sciences*, *6*, 463–476.

Herman, F., Seward, D., Valla, P. G., Carter, A., Kohn, B., Willett, S. D., & Ehlers, T. A. (2013). Worldwide acceleration of mountain erosion under a cooling climate. *Nature*, *504*(7480), 423–426. https://doi.org/10.1038/nature12877

Hickman, R. G., Dobson, P. F., Van Gerven, M., Sagala, B. D., & Gunderson, R. P. (2004). Tectonic and stratigraphic evolution of the Sarulla graben geothermal area, North Sumatra, Indonesia. *Journal of Asian Earth Sciences*, *23*(3), 435–448. https://doi.org/10.1016/s1367-9120(03)00155-x

Huchon, P., & LePichon, X. (1984). Sunda Strait and central Sumatra fault. *Geology*, *12*(11), 668–672. https://doi.org/10.1130/0091-7613(1984)12<668:ssacsf>2.0.co;2

Ito, T., Gunawan, E., Kimata, F., Tabei, T., Simons, M., Meilano, I., et al. (2012). Isolating along-strike variations in the depth extent of shallow creep and fault locking on the northern Great Sumatran Fault. *Journal of Geophysical Research*, *117*(B6), B06409. https://doi.org/10.1029/2011jb008940

Karig, D., Suparka, S., Moore, G., & Hehanussa, P. (1979). Structure and Cenozoic evolution of the Sunda arc in the central Sumatra region. *AAPG Memoir*, *29*, 223–237.

Lassal, O., Huchon, P., & Harjono, H. (1989). Extension crustale dans ledetroit de la Sonde (Indonesie): Donnees de la sismique reflexion (campagne Krakatau). *Geophysics*, *309*(2), 205–212.

Malod, J. A., & Kemal, B. M. (1996). *The Sumatra margin: Oblique subduction and lateral development of the accretionary prism* (Vol. 106, pp. 19–28). Geological Society of London Special Publication.

McCaffrey, R. (1991). Slip vectors and stretching of the Sumatran fore arc. *Geology*, *19*(9), 881–884. https://doi.org/10.1130/0091-7613(1991)019<0881:svasot>2.3.co;2

McCaffrey, R. (1992). Oblique plate convergence, slip vectors, and forearc deformation. *Journal of Geophysical Research*, *97*(B6), 8905–8915. https://doi.org/10.1029/92jb00483

McCaffrey, R. (2009). The tectonic framework of the Sumatran subduction zone. *Annual Review of Earth and Planetary Sciences*, *37*(1), 345–366. https://doi.org/10.1146/annurev.earth.031208.100212

Moore, G. F., & Curray, J. R. (1980). Structure of the Sunda Trench lower slope off Sumatra from multichannel seismic reflection data. *Marine Geophysical Researches*, *4*(3), 319–340. https://doi.org/10.1007/bf00369106

Morley, C. K., & Alvey, A. (2015). Is spreading prolonged, episodic or incipient in the Andaman Sea? Evidence from deepwater sedimentation. *Journal of Asian Earth Sciences*, *98*, 446–456. https://doi.org/10.1016/j.jseaes.2014.11.033

Morley, C. K., Chantraprasert, S., Chenoll, K., Sootlek, P., & Jitmahantakul, S. (2022). *Interaction of thin-skinned detached faults and basement-involved strike-slip faults on a transform margin: The Moattama Basin* (p. 524). Geological Society, London, Special Publications. https://doi.org/10.1144/SP524-2021-90

Morley, R. J. (2018). Assembly and division of the South and South-East Asian flora in relation to tectonic and climate change. *Journal of Tropical Ecology*, *34*(4), 209–234. https://doi.org/10.1017/s0266467418000202

Morley, R. J., Morley, H. P., & Swiecicki, T. (2016). Mio-Pliocene palaeogeography, uplands and river systems of the Sunda Region based on mapping within a framework of VIM depositional cycles. In *Proceedings, Indonesian petroleum association* (pp. IPA16–506). Fortieth Annual Convention & Exhibition.

Mukti, M. M., Maulin, H. B., & Permana, H. (2021). Growth of forearc highs and basins in the oblique Sumatra subduction system. *Petroleum Exploration and Development*, *48*(3), 683–692. https://doi.org/10.1016/s1876-3804(21)60054-x

Natawidjaja, D. H. (2018). Updating active fault maps and sliprates alone the Sumatran Fault Zone, Indonesia. *Earth and Environmental Science*, *118*, 012001. https://doi.org/10.1088/1755-1315/118/1/012001

Natawidjaja, D. H., Bradley, K., Daryono, M. R., Aribowo, S., & Herrin, J. S. (2017). Late quaternary eruption of the Ranau Caldera and new geological slip rates of the Sumatran fault zone in southern Sumatra. *Indonesia Geoscience Letters*, *21*, 4.

Prawirodirdjo, L., Bock, Y., Genrich, J. F., Puntodewo, S. S. O., Rais, J., Subarya, C., & Sutisna, S. (2000). One century of tectonic deformation along the Sumatran fault from triangulation and GPS surveys. *Journal of Geophysical Research*, *105*(B12), 28343–28361. https://doi.org/10.1029/2000jb900150

Pubellier, M., & Morley, C. K. (2014). The basins of Sundaland (SE Asia): Evolution and boundary conditions. *Marine and Petroleum Geology*, *58*, 555–578. https://doi.org/10.1016/j.marpetgeo.2013.11.019

Raju, K. A. K., Ramprasad, T., Rao, B. R., & Varghese, J. (2004). New insights into the tectonic evolution of the Andaman Basin, northeast Indian Ocean. *Earth and Planetary Science Letters*, *221*(1–4), 145–162. https://doi.org/10.1016/s0012-821x(04)00075-5

Sieh, K., Bock, Y., Edwards, L., Taylor, F., Gans, P., & Zachariasen, J. (1994). Active tectonics of Sumatra. *Geological society of America* (Vol. 26). GSA abstracts with programs. A-382.

Sieh, K., & Natawidjaja, D. (2000). Neotectonics of the Sumatran fault, Indonesia. *Journal of Geophysical Research*, *105*(B12), 28295–28326. https://doi.org/10.1029/2000jb900120

Simons, W. J. F., Socquet, A., Vigny, C., Ambrosius, B. A. C., Haji, A. S., Promthong, C., et al. (2007). A decade of GPS in Southeast Asia: Resolving Sundaland motion and boundaries. *Journal of Geophysical Research*, *112*(B6), B06420. https://doi.org/10.1029/2005jb003868

Stockli, D. F., Farley, K. A., & Dumitru, T. A. (2000). Calibration of the apatite (U-Th)/He thermochronometer on an exhumed fault block, White Mountains, California. *Geology*, *28*(11), 983–986. https://doi.org/10.1130/0091-7613(2000)28<983:cotaht>2.0.co;2

Tingay, M., Morley, C., King, R., Hillis, R., Coblentz, D., & Hall, R. (2010). Present-day stress field of Southeast Asia. *Tectonophysics*, *482*(1–4), 92–104. https://doi.org/10.1016/j.tecto.2009.06.019

Wang, W., Zheng, D., Li, C., Wang, Y., Zhang, Z., Pang, J., et al. (2019). Cenozoic exhumation of the Qilian Shan in the northeastern Tibetan Plateau: Evidence from low-temperature thermochronology. *Tectonics*, *39*(4), e2019TC005705. https://doi.org/10.1029/2019tc005705

Yeats, R. S., Sieh, K., & Allen, C. R. (1997). *The Geology of Earthquakes* (p. 568). Oxford: Oxford University. Press.

Zaim, Y., Habrianta, L., Abdullah, C. I., AswanRizal, Y., Basuki, N. I., & Sitorus, F. E. (2012). Depositional history and petroleum potential of Ombilin Basin, West Sumatra- Indonesia, based on surface geological data. Search and discovery Article 10449 (p. 8).

References From the Supporting Information

Flowers, R. M., Ketcham, R. A., Shuster, D. L., & Farley, K. A. (2009). Apatite (U-Th)/He thermochronometry using a radiation damage accumulation and annealing model. *Geochimica et Cosmochimica Acta*, *73*(8), 2347–2365. https://doi.org/10.1016/j.gca.2009.01.015

Willett, S. D., & Brandon, M. T. (2013). Some analytical methods for converting thermochronometric age to erosion rate. *Geochemistry, Geophysics, Geosystems*, *14*(1), 209–222. https://doi.org/10.1029/2012gc004279